

Effect of large neutron excess on the dipole response in the region of the Giant Dipole Resonance

F. Catara ^{a,d}, E.G. Lanza ^a, M.A. Nagarajan ^{b,1} and A. Vitturi ^c

^a *Dipartimento di Fisica and INFN, Catania, Italy*

^b *Laboratori Nazionali di Legnaro, INFN, Italy*

^c *Dipartimento di Fisica and INFN, Padova, Italy*

^d *Departamento de Fisica Atomica, Molecular y Nuclear, Sevilla, Spain*

Abstract

The evolution of the Dipole Response in nuclei with strong neutron excess is studied in the Hartree-Fock plus Random Phase Approximation with Skyrme forces. We find that the neutron excess increases the fragmentation of the isovector Giant Dipole Resonance, while pushing the centroid of the distribution to lower energies beyond the mass dependence predicted by the collective models. The radial separation of proton and neutron densities associated with a large neutron excess leads to non vanishing isoscalar transition densities to the GDR states, which are therefore predicted to be excited also by isoscalar nuclear probes. The evolution of the isoscalar compression dipole mode as a function of the neutron excess is finally studied. We find that the large neutron excess leads to a strong concentration of the strength associated with the isoscalar dipole operator $\sum_i r_i^3 Y_{10}$, that mainly originates from uncorrelated excitations of the neutrons of the skin.

Currently, there has been interest in the study of the effect of neutron skin on collective states in neutron-rich nuclei [1–4]. One of the collective modes of interest is the Isovector Giant Dipole resonance (GDR) in such nuclei. In neutron-rich nuclei, one expects the neutron and proton densities to have different shapes. This would allow the possibility of exciting the isovector GDR by isoscalar probes through hadronic interactions [5–7], in addition to the usual method through Coulomb excitation [8]. The excitation of the isovector GDR by isoscalar probes through hadronic interactions is possibly the most sensitive measure of the “neutron skin”. This property can be assessed by the evaluation of the isoscalar and isovector dipole transition densities in neutron-rich nuclei.

¹ Current address: Department of Physics, UMIST, Manchester M60 IQD, UK

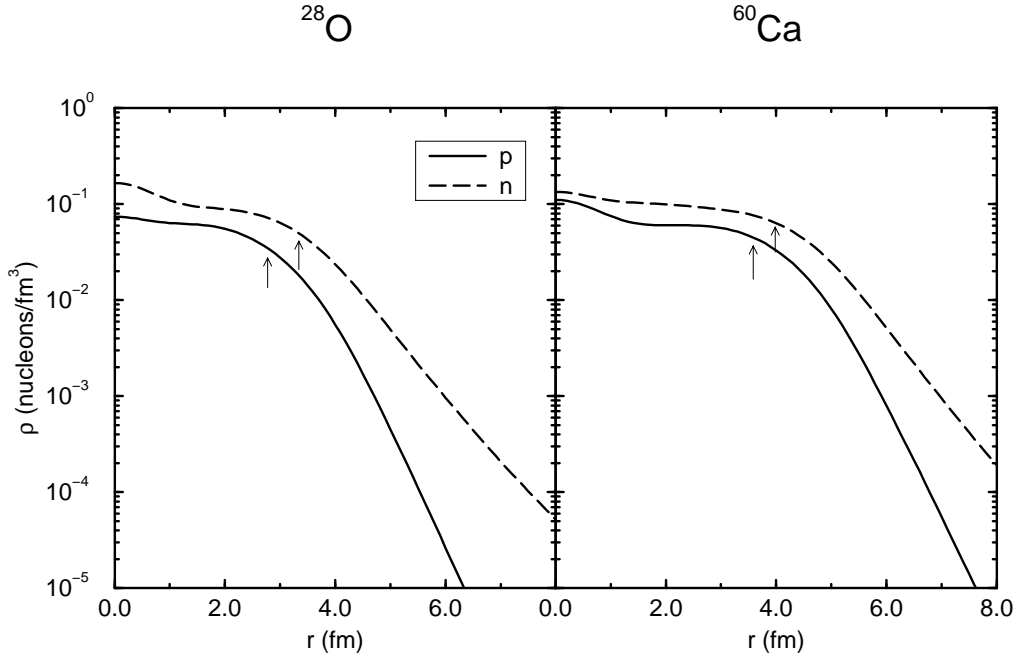


Fig. 1. Hartree-Fock proton and neutron densities obtained for ^{28}O and ^{60}Ca with SGII interaction. The arrows indicate the r.m.s. radii.

In order to investigate the effect of neutron skin on collective dipole states of neutron-rich nuclei, we have performed microscopic calculations for several isotopes of oxygen and calcium nuclei, based on spherical Hartree-Fock (HF) method with Skyrme SGII interaction. The proton and neutron densities in ^{28}O and ^{60}Ca are shown in Fig. 1. The HF calculations predict the last neutron to be bound by 3.25 MeV in ^{28}O and 5.1 MeV in ^{60}Ca . These relatively large values of the neutron separation energy hinder the occurrence of “unusual” concentration of dipole strength at the continuum threshold, an effect that is directly associated with very small binding energy [3,9]. Note that the use of other Skyrme interactions may give rather smaller neutron separation energy, leading to different features in the very low energy part of the response. This should not alter the medium and high energy regions, which are the object of the present investigation.

The collective dipole excitations of these nuclei were calculated in RPA, using the full residual interaction. After obtaining the dipole states by the RPA calculation, we calculated the response to the isovector dipole operator $\sum_i z_i \tau_i^3$. Similarly we can calculate the isoscalar response to the operator $\sum_i z_i$, which should vanish if the RPA states were proper eigenstates of a translationally invariant hamiltonian, together with the occurrence at zero excitation energy of the spurious state. Since the last neutrons in these nuclei are not too weakly bound, the continuum states needed for the RPA were expanded in oscillator functions of different principal quantum number, a procedure which was found to be adequate in these systems. In actual RPA calculations, because

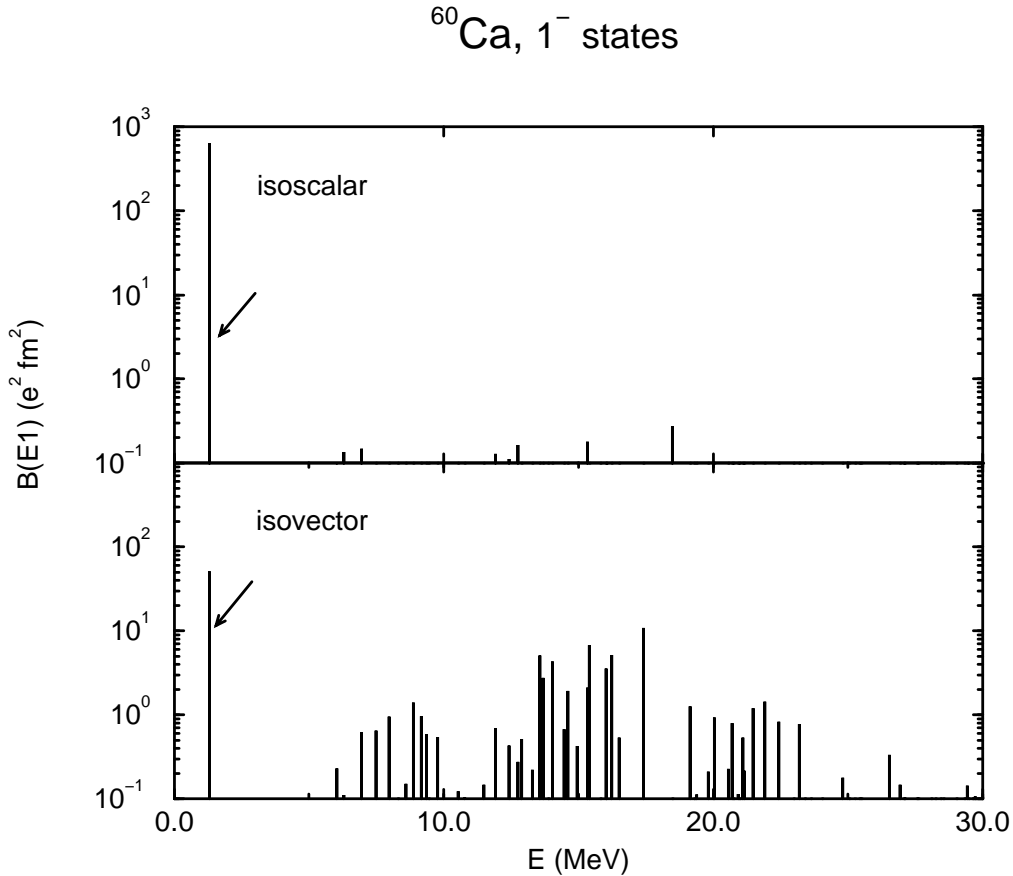


Fig. 2. Isoscalar and isovector dipole response obtained in HF+RPA for ^{60}Ca . Most of the spurious isoscalar response is concentrated in one low-lying state which can be easily eliminated.

of the truncation involved and the additional effect of the isospin mixing introduced by the Coulomb interaction, the spurious isoscalar mode occurs at very low excitation energy (carrying a large fraction of its strength) and there are insignificant spurious center-of-mass components at higher energies. The spurious state can thus be eliminated.

An example of the calculated $B(E1)$'s for isoscalar and isovector dipole strength distributions is shown for ^{60}Ca in Fig. 2. The spurious state occurring at low excitation energy is marked with an arrow.

In view of the interest in the effect of neutron excess on the isovector dipole states, the RPA results of the different oxygen and calcium isotopes are shown in Fig. 3. One of the effects of the neutron excess is the spreading of the isovector dipole strength. It should be noted that in both the ^{28}O and ^{60}Ca cases, the most “collective” state only exhausts approximately 15 % of the total EWSR. The increased spreading in the neutron rich isotopes is more clearly seen in Fig. 4, where we have averaged the dipole response with a lorentzian with a width of 2 MeV. In both cases the full width at half maximum

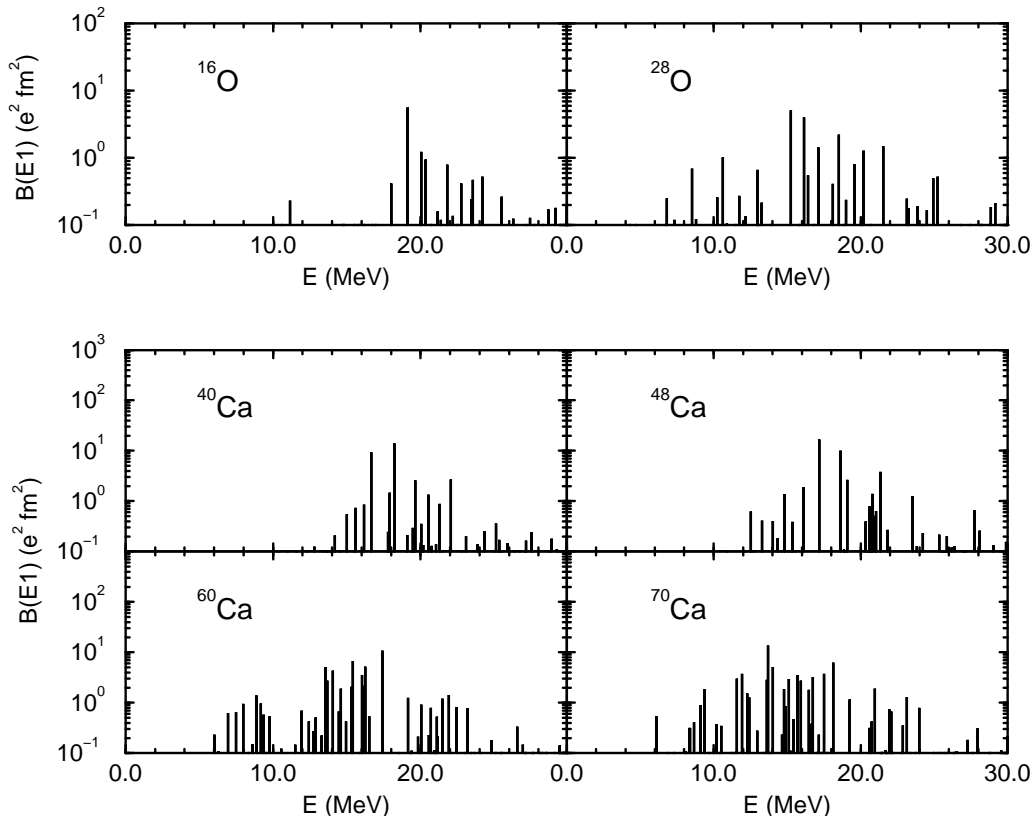


Fig. 3. Isovector dipole response obtained in HF+RPA for a sequence of Oxygen and Calcium isotopes. Spurious states have been eliminated (cf. Fig. 2).

(FWHM) is seen to have increased by about 50 % going from the $N=Z$ to the most neutron rich isotope. In addition, one observes that the centroid of the strength function shifts to lower energy in the neutron rich isotopes. This shift is larger than can be accounted by the $A^{-1/6}$ dependence given by the Goldhaber-Teller [10] model. For example the centroid changes from 19 MeV in ^{40}Ca to 16 MeV in ^{60}Ca , a shift which is a factor two larger than the prediction of the Goldhaber-Teller model. The shift is closer, although still slightly larger, to the prediction of the $A^{-1/3}$ scaling associated with the hydrodynamical model [11].

Even though the isoscalar $B(E1)$ to all states must identically vanish, the corresponding isoscalar transition densities to the different states need not to be identically zero. For example, within the collective Goldhaber-Teller model for the GDR, only in the particular case where the neutron and proton densities have the same shape (and scale with N and Z) would the isoscalar dipole transition density vanish. If the neutron and proton transition densities have different shapes, as is the case for very neutron rich nuclei, the corresponding isoscalar dipole transition density will be non zero. The isoscalar and isovector-dipole transition densities to a selected state in ^{28}O and ^{60}Ca are shown in Fig. 5. The states selected have 18 and 17.4 MeV of excitation energy and carry 8 and 16 % of the EWSR, respectively. In these figures also are shown the separate neutron and proton transition densities.

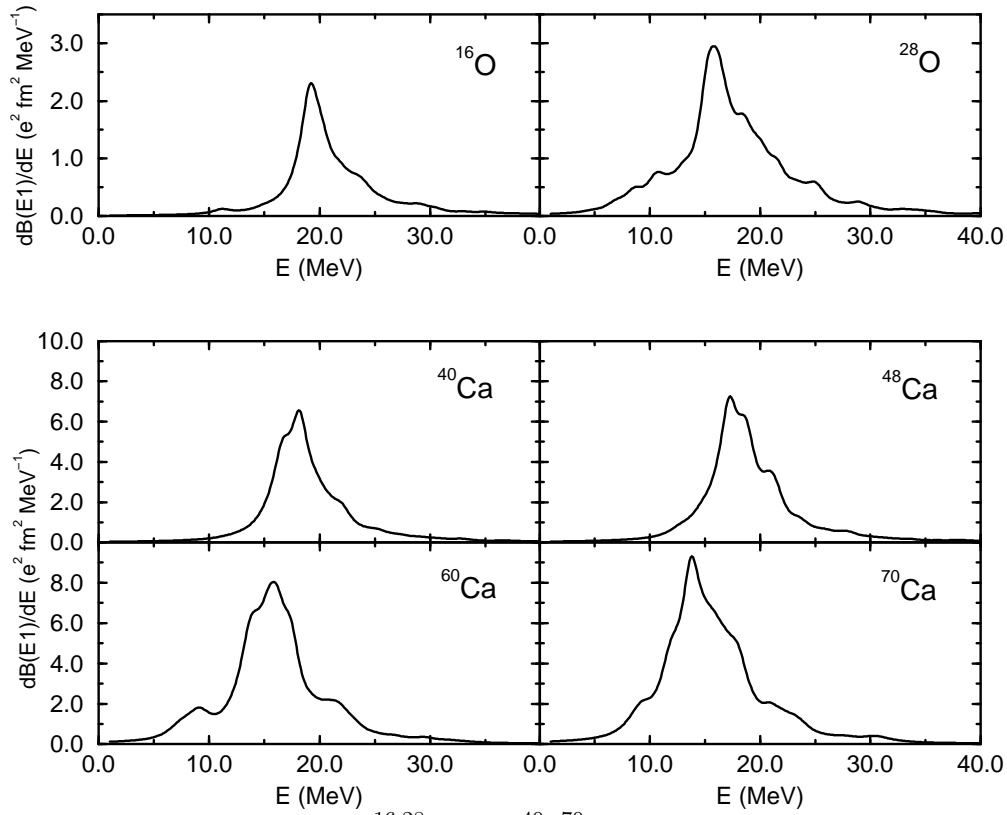


Fig. 4. Dipole response for $^{16,28}\text{O}$ and $^{40-70}\text{Ca}$ obtained from the RPA response shown in Fig. 3, by averaging the discrete spectra with a lorentzian with $\Gamma=2$ MeV.

We can compare the microscopic transition densities with those predicted by the macroscopic Goldhaber-Teller transition density

$$\delta\rho_{GDR}^{isoscalar}(r) = \delta\rho_{GDR}^p + \delta\rho_{GDR}^n = \alpha_1 \left[\frac{2N}{A} \frac{d\rho_p}{dr} - \frac{2Z}{A} \frac{d\rho_n}{dr} \right]$$

where α_1 , given by

$$\alpha_1^2 = \frac{\pi\hbar^2}{2m} \frac{A}{NZE_x}$$

is the amplitude of the oscillation, derived from the dipole EWSR. E_x is the excitation energy of the dipole state and it is assumed that the state exhausts the full EWSR. The features of this isoscalar transition density can be better evidenced by expanding it in the neutron excess parameter, according to Satchler [7], in the form

$$\delta\rho_{GDR}^{isoscalar}(r) \approx \alpha_1\gamma \left(\frac{N-Z}{A} \right) \left[\frac{d\rho(r)}{dr} + \frac{R_0}{3} \frac{d^2\rho(r)}{dr^2} \right]$$

where $R_0 = (R_n + R_p)/2$ is the average radius of the total nuclear density $\rho(r)$ and the parameter γ is related by $\gamma(N-Z)/A = 3/2 (\Delta R/R_0)$ to the measure of the neutron skin $\Delta R = R_n - R_p$. The isoscalar transition density is therefore, to leading order, directly proportional to the neutron skin.

The corresponding isovector transition density has a weaker dependence on

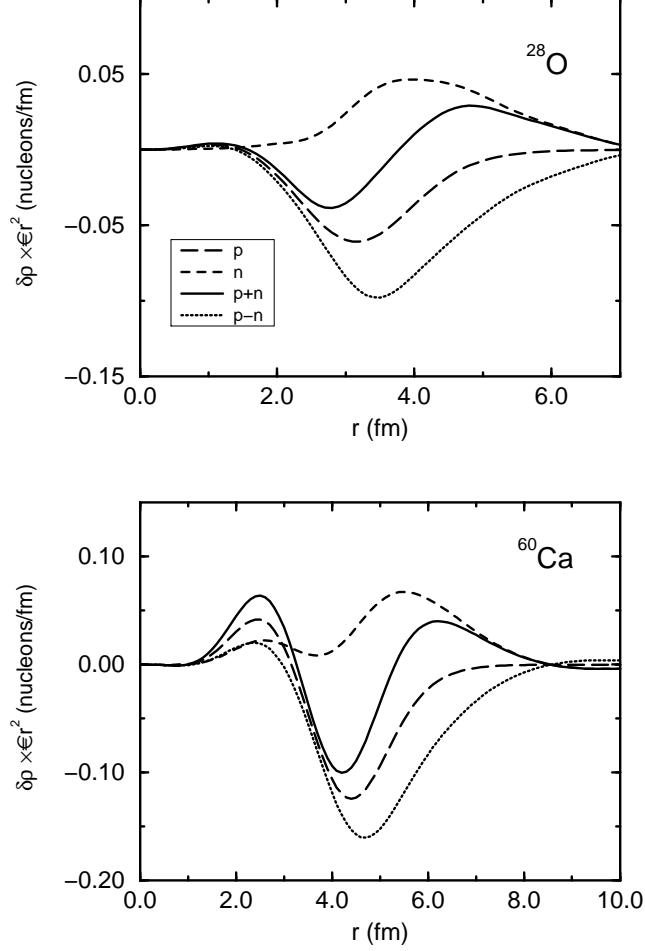


Fig. 5. Transition densities to selected RPA states. Both isoscalar and isovector densities are shown, together with the separate proton and neutron contributions. The states selected in ^{28}O and ^{60}Ca have 18 and 17.4 MeV of excitation energy and carry 8 and 16 % of the EWSR, respectively. All densities are multiplied by r^2 .

the neutron excess, to first order in $\Delta R/R_0$ and $(N - Z)/A$, given by

$$\begin{aligned} \delta\rho_{GDR}^{isovector}(r) &= \delta\rho_{GDR}^n - \delta\rho_{GDR}^p \\ &= -\alpha_1 \left[\frac{2N}{A} \frac{d\rho_p}{dr} + \frac{2Z}{A} \frac{d\rho_n}{dr} \right] \approx -\alpha_1 \frac{4NZ}{A^2} \frac{d\rho(r)}{dr} \end{aligned}$$

In Fig. 6, we show the comparison between the microscopic transition densities and the macroscopic ones for the state in ^{28}O , already illustrated in Fig. 5. The amplitude α_1 of the macroscopic model has been rescaled according to the proper percentage of the EWSR exhausted by the state. Both the

^{28}O , Dipole

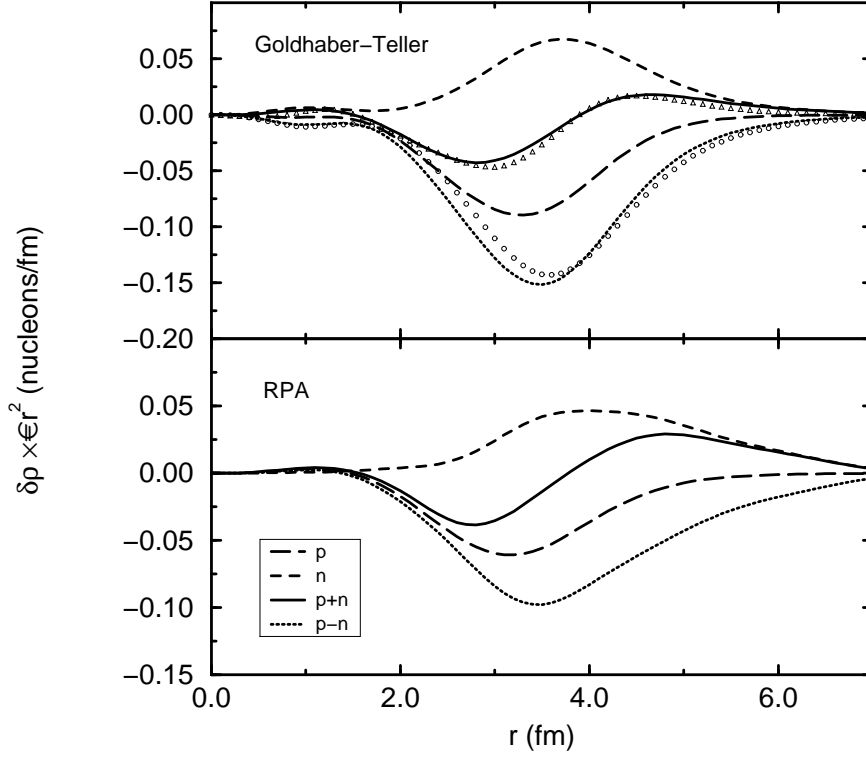


Fig. 6. Comparison of the microscopic proton and neutron transition densities and their isoscalar and isovector combinations (lower part) with the corresponding macroscopic expressions obtained within the Goldhaber-Teller model (upper part). The figure refers to the state in ^{28}O , shown in Fig. 5. We also show in the upper figure as curves with triangles and circles the approximated expression of Satchler for the isoscalar and isovector transition densities, respectively. In this approximate expressions, a value $\Delta R/R = 0.186$ was used, taken from the HF density calculation.

“exact” Goldhaber-Teller expressions and the approximated forms suggested by Satchler are used (note that these latter practically coincide with the exact ones). One can see from the comparison that the relevant features of the microscopic RPA transition density are well reproduced by the collective GT model.

One can observe from Figs. 5 and 6 the occurrence in the case of very neutron-rich systems of a node in the isoscalar transition density at the nuclear surface. Furthermore, at large radii both the isoscalar and isovector densities have similar radial dependence and magnitude. This is a reflection of the fact that in this region it is only the tail of the neutron density that contributes and thus both isoscalar and isovector components contribute equally in this region.

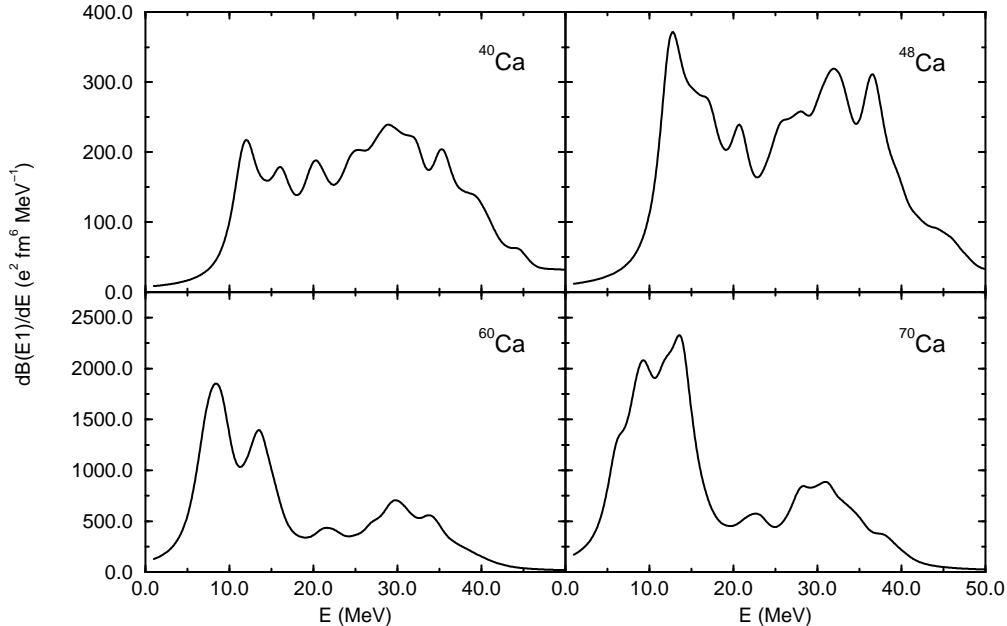


Fig. 7. Isoscalar dipole response to the RPA states obtained using the operator $\sum_i z_i r_i^2$, for a sequence of Calcium isotopes, after averaging the discrete spectra with a lorentzian with $\Gamma=3$ MeV.

The fact that the isoscalar dipole transition density has different sign at small and large radii has the consequence that the Coulomb-nuclear interference will be destructive at small radii and constructive at larger radii beyond the node. This has been pointed out by several authors [5–7] and this feature has been exploited as a specific tool in order to obtain a measure of the neutron skin [12,13].

Finally, we consider the possible compressional Isoscalar Dipole Resonance (IDR) which is generated by the operator $\sum_i z_i r_i^2$. This operator is the leading non-spurious term in the expansion of $j_1(qr)Y_{10}(\hat{r})$ in the electromagnetic field. The excitation of this isoscalar giant dipole resonance via inelastic scattering of α particles has been investigated in ref. [14], and the model has been developed and compared to microscopic RPA calculations in ref. [15], who considered systems with different masses in the stability region. In Fig. 7, we present the evolution of the response for this operator in RPA with increasing number of neutrons, considering the sequence of isotopes $^{40,48,60,70}\text{Ca}$. It can be observed that there is an increased strength in the response as one moves to neutron-rich nuclei, approximately according to the "standard" $A^{7/3}$ scaling predicted by the EWSR. The neutron skin has in fact only a mild effect on the total EWSR, which is given by [14–16]

$$EWSR = \frac{\hbar^2 A}{8m\pi} \left[11\langle r^4 \rangle - \frac{25}{3}\langle r^2 \rangle^2 \right]$$

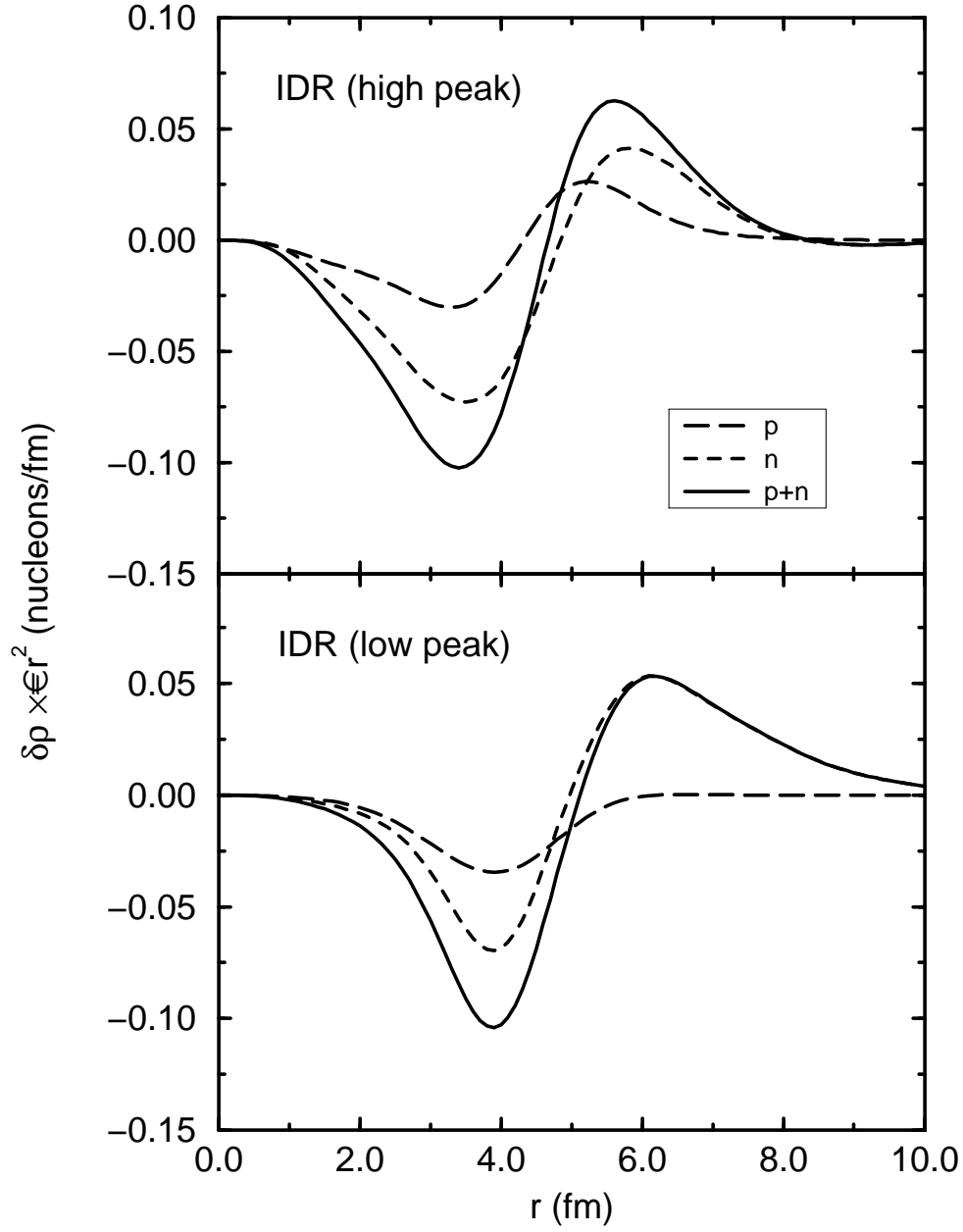


Fig. 8. Isoscalar transition densities to the selected states in ^{60}Ca collecting a large fraction of the isoscalar dipole strength. The state in the upper part ($E=31.3$ MeV) belongs to the high-energy peak of the strength distribution, the one in the lower part ($E=9.4$ MeV) to the low-energy peak. The isoscalar transition densities are shown together with the separate proton and neutron components.

and which can be in leading order estimated to be

$$EWSR \approx \frac{3\hbar^2 r_0^4}{14m\pi} A^{7/3} \left(1 + 2 \frac{N - Z}{A} \frac{\Delta R}{R} \right)$$

So, even in the extreme case of ^{70}Ca , the correction over the $A^{7/3}$ scaling is of the order of few percent. On the other hand, aside from the EWSR, the large neutron excess seems to have dramatic effects on the energy distribution of the strength. While, in fact, along the stability valley the increased mass is just shifting the collective peak to lower energies approximately according to a $150A^{-1/3}$ law [15], in this case a splitting of the strength in two main components occurs. The lower one, which is associated with the excitation of the neutrons of the skin, becomes progressively more pronounced as one approaches the drip line.

This feature is better evidenced by the corresponding transition densities. We show in Fig. 8 the transition density for a state in the low-energy peak and one in the high-energy peak. In the former case the neutron contribution is completely dominant and the transition density has a longer tail as expected for a contribution involving weakly bound particles of the skin. In the latter case the neutron and proton components are comparably important, and they decay faster in the tail and they are peaked at smaller distances, according to the fact that they correspond to excitation of particles of the core.

To summarize, we have studied within HF plus RPA with Skyrme interaction the effects of increasing neutron excess on the isovector Giant Dipole Resonance and on the compressional Isoscalar Dipole Resonance. For the former we have found an increasing fragmentation of the strength distribution when moving towards the drip line, together with a shift to lower energies larger than the mass dependence prediction based on collective models. For the latter, associated with the isoscalar dipole operator $\sum_i z_i r_i^2$, a strong concentration of the strength at low energy (around 10 MeV) has been found for large neutron excess. This is interpreted as arising from the excitation involving the neutrons of the skin.

Acknowledgements

One of us (F.C.) is grateful to the Departamento de FAMN of the University of Sevilla for the warm hospitality during his stay made possible by grant n^o ERBFMBICT-961042 by the European Community within the TMR program.

References

- [1] T. Otsuka, A. Muta, M. Yokoyama, N. Fukimishi and T. Suzuki, Nucl. Phys. A588 (1995) 113c.
- [2] I. Hamamoto and H. Sagawa, Phys. Rev. C53 (1996) R1493.
- [3] I. Hamamoto, H. Sagawa and X.Z. Zhang, Phys. Rev. C53 (1996)765.
- [4] F. Catara, E.G. Lanza, M.A. Nagarajan and A. Vitturi, Nucl. Phys. A614 (1997) 86.
- [5] S. Shlomo, Y.W. Lui, D.H. Youngblood, T. Udagawa and T. Tamura, Phys. Rev. C36 (1987) 1317.
- [6] K. Nakayama and G. Bertsch, Phys. Rev. Lett. 59 (1987) 1053.
- [7] G.R. Satchler, Nucl. Phys. A472 (1987) 215.
- [8] P. Decowski and H.P. Morsch, Nucl. Phys. A377 (1982) 261.
- [9] H. Sagawa et al. , Z. Phys. A351 (1995)385; F. Catara, C.H. Dasso and A. Vitturi, Nucl. Phys. A602 (1996) 181.
- [10] M. Goldhaber and E. Teller, Phys. Rev. 74 (1948) 1046.
- [11] H. Steinwedel and J.H.D. Jensen, Z. Naturforsch. 5a (1950) 413.
- [12] A. Krasznahorkay et al. , Nucl. Phys. A567 (1994) 521.
- [13] C.H. Dasso et al., to be published
- [14] M.N. Harakeh and A.E.L. Dieperink, Phys. Rev. C23 (1981) 2329.
- [15] N. Van Giai and H. Sagawa, Nucl. Phys. A371 (1981) 1.
- [16] E. Lipparini and S. Stringari, Phys. Rep. 175 (1989) 103.